University of Glasgow | Experimental Particle Physics

**GLAS-PPE/2009-24**
23rd November 2009

Department of Physics and Astronomy
Experimental Particle Physics Group
Kelvin Building, University of Glasgow,
Glasgow, G12 8QQ, Scotland
Telephone: +44 (0)141 330 2000 Fax: +44 (0)141 330 5881

# Reconstruction of the decay modes $B_d^0 \to D_d^{\pm}\pi^{\mp}$, $B_s^0 \to D_s^-\pi^+$, and $B_s^0 \to D_s^{\pm}K^{\mp}$ at LHCb

V. V. Gligorov[1]

[1] CERN, Geneva and University of Glasgow, Glasgow, G12 8QQ, Scotland

**Abstract**

This note describes a unified approach to the reconstruction of the decay modes $B_d^0 \to D_d^{\pm}\pi^{\mp}$, $B_s^0 \to D_s^-\pi^+$, and $B_s^0 \to D_s^{\pm}K^{\mp}$ within the DC06 simulation framework for LHCb. The expected signal yield after the offline selection and the first-level hardware trigger in 2 fb$^{-1}$ of data is $(1.23 \pm 0.08) \cdot 10^6$ events for $B_d^0 \to D_d^{\pm}\pi^{\mp}$, $(1.7 \pm 0.5) \cdot 10^5$ events for $B_s^0 \to D_s^-\pi^+$, and $(1.4 \pm 0.5) \cdot 10^4$ events for $B_s^0 \to D_s^{\pm}K^{\mp}$.

Table 1: The branching ratios for the signal modes used in this study. The branching ratio quoted for the decay mode $B_s^0 \to D_s^\pm K^\mp$ is obtained by multiplying the CDF measurement [1] of the relative branching ratio for the modes $B_s^0 \to D_s^\pm K^\mp$ and $B_s^0 \to D_s^- \pi^+$ by the latest measurement of the $B_s^0 \to D_s^- \pi^+$ branching ratio published in the PDG [2]. The statistical and systematic uncertainties on the measurement of the relative branching ratio ($0.107 \pm 0.019 \pm 0.008$) are added quadrature to obtain an overall uncertainty on the relative branching ratio, which is subsequently added in quadrature with the uncertainty on the $B_s^0 \to D_s^- \pi^+$ branching ratio.

| Decay mode | Branching ratio (B.R.) |
|---|---|
| $B_d^0 \to D_d^\pm \pi^\mp$ | $(2.47 \pm 0.13) \cdot 10^{-4}$ |
| $B_s^0 \to D_s^- \pi^+$ | $(1.8 \pm 0.5) \cdot 10^{-4}$ |
| $B_s^0 \to D_s^\pm K^\mp$ | $(1.9 \pm 0.7) \cdot 10^{-5}$ |

# 1 Introduction

Charmed hadronic decays of neutral $B_d$ and $B_s$ mesons are sensitive to a wide range of physics parameters of interest to flavour physics, and their large branching ratios and distinctive decay topologies make these modes interesting both for early measurements and long-term precision studies. In particular, the family of decay modes

$$B_d^0 \to D_d^\pm \pi^\mp, B_s^0 \to D_s^- \pi^+, B_s^0 \to D_s^\pm K^\mp,$$

is sensitive to the CKM angle $\gamma$, the mass differences in the $B_{s,d}^0$ systems $\Delta m_{s,d}$, and the $B_s^0$ lifetime difference $\Delta\Gamma_s$. They are also of particular interest for the precision measurement of the ratio of $B_s$ and $B_d$ lifetimes because of the large expected yields of the highest branching ratio modes $B_d^0 \to D_d^\pm \pi^\mp$ and $B_s^0 \to D_s^- \pi^+$. Both the reconstruction of these decay modes [3, 4, 5] and the exploitation of their physics potential [6, 7, 8, 9, 10] have been studied extensively at LHCb. This note presents a unified approach to the reconstruction of these decay modes under the assumption that the charmed meson decays into the Cabbibo-favoured combination of three charged hadrons: $D_d^\pm \to K^\mp \pi^\pm \pi^\pm$ and $D_s^\pm \to K^\mp K^\pm \pi^\pm$.

For the reader's convenience, the branching ratios for the relevant signal modes (multiplied by the branching ratios for the relevant $D_{d,s}^\pm$ decays) are listed in Table 1. Unless explicitly stated otherwise, all branching ratios quoted throughout this note are the latest values published by the Particle Data Group [2]. For the sake of brevity, the three decays

$$B_d^0 \to D_d^\pm \pi^\mp, B_s^0 \to D_s^- \pi^+, B_s^0 \to D_s^\pm K^\mp,$$

will be collectively referred to as $B_{d,s}^0 \to D_{d,s}^\pm (\pi, K)^\mp$ from now on.

A unified approach to the selection of these decay modes is desirable because the channels in question have identical[1)] kinematics and decay topologies. They are distinguished through particle identification (PID) cuts, defined in Section 3, and mass cuts. Since the kinematic and topological cuts do not distinguish one $B_{d,s}^0 \to D_{d,s}^\pm (\pi, K)^\mp$ decay mode from another, all decays in this family ought to be reconstructed using a single set of kinematic cuts. The only caveat is that lower branching ratio channels should use proportionally tighter cut values (within the same set of cuts) to achieve the required suppression of combinatoric background. As an example, consider a simultaneous fit to the CKM angle $\gamma$, the $B_s^0$ mass difference $\Delta m_s$, and the $B_s^0$ lifetime difference $\Delta\Gamma_s$ using the decay modes $B_s^0 \to D_s^\pm K^\mp$ and $B_s^0 \to D_s^- \pi^+$. As will be seen in Section 5.4.2, the decay mode $B_s^0 \to D_s^- \pi^+$ is one of the major sources of background to the decay mode $B_s^0 \to D_s^\pm K^\mp$, and this background level must be accounted for correctly in the simultaneous fit. A unified selection makes this simple, as there is no need to account for different kinematic cuts, and the full power of the PID and mass information can be used within the simultaneous fit likelihood to produce an event-by-event signal (background) probability.

Section 2 summarizes the previous studies of these channels at LHCb. Section 3 explains some LHCb-specific terminology used in this note. Section 4 describes the current LHCb trigger. Section 5 discusses the offline selection of these decay modes. Section 7 presents the conclusions of this study. Natural units are used throughout.

[1)] Apart from minor effects due to the kaon-pion mass difference.

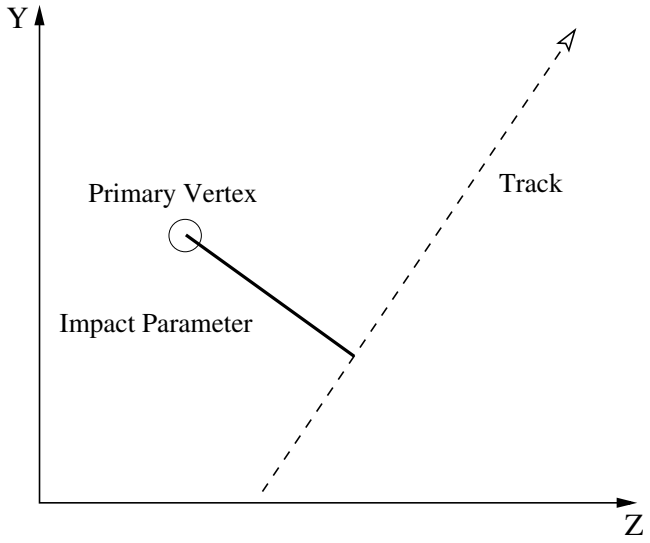


Figure 1: The 2D impact parameter of a track with respect to a vertex.

## 2 Summary of previous studies

This note builds on a number of previous studies of the reconstruction and physics exploitation of the decay modes $B^0_{d,s} \to D^{\pm}_{d,s}(\pi, K)^{\mp}$. Aside from the unified approach, the main difference between the work in this note and previous studies is that the software simulation of LHCb has undergone significant changes in the meantime. The new simulation is more realistic with respect to the final detector geometry [11], includes improved descriptions of detector response and makes use of the latest reconstruction algorithms. Adopting standard LHCb terminology, studies carried out with the old simulation will be referred to as DC04 studies throughout this note, while studies carried out with the new simulation will be referred to as DC06 studies.

Three decay modes were studied with the DC04 simulation: $B^0_d \to D^{\pm}_d\pi^{\mp}$, $B^0_s \to D^{\pm}_s K^{\mp}$, and $B^0_s \to D^-_s\pi^+$. In the case of $B^0_d \to D^{\pm}_d\pi^{\mp}$, the event reconstruction and selection [5] was optimized for the purpose of extracting the CKM angle $\gamma$ [7]. In the case of $B^0_s \to D^{\pm}_s K^{\mp}$ and $B^0_s \to D^-_s\pi^+$, a unified selection was studied [4] and the extraction of the CKM angle $\gamma$ using all three decay modes in a combined fit was also studied [7].

Although this note presents results obtained using the DC06 simulation of the LHCb detector, not all datasets studied were produced and processed using the same reconstruction and selection software. These discrepancies will be discussed in more detail in those instances where they lead to noticeable differences in performance.

## 3 Terminology

As an aid to the reader, some of the less obvious variables used in the selection and their acronyms are now defined.

- **Impact parameter :** The impact parameter (IP) of a track with respect to a vertex is defined as the perpendicular distance between the track and the vertex. Figure 1 shows this graphically in two dimensions; the actual IP values used in this selection are calculated in three dimensions. The IP $\chi^2$ is used to cut on in DC06, whereas the IP significance (IPs), defined as the IP divided by its uncertainty, was used in DC04. The two quantities are highly correlated and to first order

$$\text{IP } \chi^2 \approx (\text{IPs})^2 . \tag{1}$$

- **DLL $K - \pi$ separation :** LHCb uses two Ring-Imaging Cherenkov (RICH) detectors [12] to identify particles. The Delta Log Likelihood (DLL) cut is the difference in the log-likelihoods of the RICH reconstructions of a track under different particle hypotheses, in this case the pion hypothesis and the kaon hypothesis. A DLL can be formed between any two mass hypotheses.

- **$D^{\pm}_{d,s}$ and $B^0_{s,d}$ mass windows :** Wide mass windows are used in the selection to provide "sidebands" to allow for a study of the background level and makeup; tight mass windows are used for the final signal yield and purity estimates.

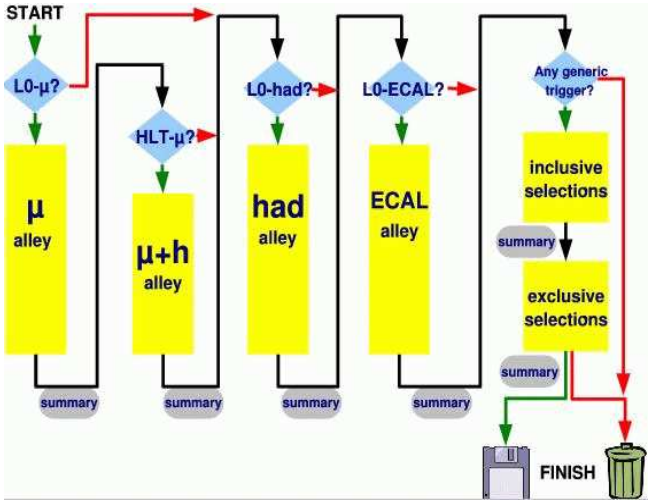


Figure 2: The new HLT, as used in the DC06 simulation. The "alleys" refer to the HLT1 stage, while the inclusive and exclusive selections refer to the HLT2 stage of the trigger.

- **Minimum flight separation from the primary vertex (abbreviated as FSPV) :** The $D^{\pm}_{d,s}$ is a relatively long lived particle (with a mean life of $\approx 1.0$ ps for the $D^{\pm}_{d}$ and $\approx 0.5$ ps for the $D^{\pm}_{s}$) and is a daughter of the $B^0_{d,s}$, itself a long-lived particle. Hence a cut on the significance of the $D^{\pm}_{d,s}$ spatial separation from the primary vertex is an excellent discriminant against background. In events which contain more than one primary vertex, the primary vertex with respect to which the $B^0_{d,s}$ has the smallest IP $\chi^2$ is used for this cut. This cut is also applied to the $B^0_{d,s}$. As with IP cuts, the $\chi^2$ of the flight separation is cut on in DC06, whereas the significance was cut on in DC04. These two quantites are related in an analogous manner to Equation 1.
- **The angle between the $B^0_{d,s}$ flight direction and momentum ($\cos\theta$) :** The direction of the $B^0_{d,s}$ momentum should be consistent with the $B^0_{d,s}$ flight direction as calculated from the vector joining the primary vertex and the $B^0_{d,s}$ decay vertex. The angle $\theta$ is defined as $\cos\theta = \frac{\mathbf{P_B}\cdot(\mathbf{DV_B}-\mathbf{PV})}{|\mathbf{P_B}||\mathbf{DV_B}-\mathbf{PV}|}$, where $\mathbf{DV_B}$ are the coordinates of the $B^0_{d,s}$ decay vertex, and $\mathbf{PV}$ are the coordinates of the primary vertex. An event at LHCb can have more than one reconstructed primary vertex. The primary vertex with respect to which the $B^0_{d,s}$ has the smallest IP $\chi^2$ is used for this cut.

# 4 LHCb trigger

The LHCb trigger has recently undergone a major redesign from the structure described in the Trigger TDR [13]. At the time of writing, no up-to-date public reference exists for the new trigger, and a brief overview of those parts most relevant to the present study must therefore be given. The LHCb trigger is rapidly evolving in response to ongoing optimization efforts, and this evolution will continue and intensify once real data is available for optimization and commissioning work. Nonetheless, it is expected that the design described here will be deployed without major architectural changes when LHCb begins data taking.

The LHCb trigger consists of three parts, utilising increasingly sophisticated event reconstructions to discriminate signal from background and reduce the LHCb bunch-crossing rate[2)] of 40 MHz to a data recording rate of 2 kHz. Of these, the first part is the Level-0 (L0) hardware trigger, while the second and third parts are software triggers collectively referred to as the High Level Trigger (HLT). The L0 trigger uses mainly information from the calorimeters and muon chambers to select events with high transverse-energy deposits, or a dimuon combination close to the $J/\psi$ mass or above $\approx 4700$ GeV. It reduces the event rate to 1 MHz. The structure of the HLT is shown in Figure 2.

The HLT is split into two parts, HLT1 and HLT2. The HLT1 stage confirms the L0 trigger decision through a set of "alleys", each of which correspond to one type of L0 decision. For example, the "hadron alley" confirms the L0 trigger decision in those cases where the L0 triggered on a high transverse energy deposit in the hadronic calorimeter by attempting to match a track to this energy deposit. The HLT1 trigger stage is the first at which lifetime biasing cuts, for example on the impact parameters of tracks, are applied. The HLT2 stage consists

[2)] Corresponding to a non-empty interaction rate of 10 MHz.

Table 2: The list of DC04 optimized cuts for the channel $B_d^0 \to D_d^{\pm}\pi^{\mp}$, taken from [5]. The DC04 yield after all triggers (in 2 fb$^{-1}$ of data at the nominal LHCb luminosity) and purity are also listed for comparison.

| Cut | Value for best $\frac{S}{\sqrt{S+B}}$ |
|---|---|
| All particle momenta | $> 2000$ MeV |
| Kaon candidate DLL K-Pi | $> 0$ |
| $D^{\pm}$ daughter $p_t$ | $> 300$ MeV |
| $D^{\pm}$ $p_t$ | $> 2000$ MeV |
| $D^{\pm}$ daughter IPs | $> 2$ |
| $D^{\pm}$ IPs | $> 3$ |
| $D^{\pm}$ mass | $\pm 21$ MeV |
| $D^{\pm}$ vertex $\chi^2$ | $< 20$ |
| $D^{\pm}$ FSPV | $> 10$ |
| Bachelor $\pi$ $p_t$ | $> 500$ MeV |
| Bachelor $\pi$ IPs | $> 2.5$ |
| $B_d^0$ mass wide | $\pm 500$ MeV |
| $B_d^0$ mass tight | $\pm 50$ MeV |
| $B_d^0$ vertex $\chi^2$ | $< 10$ |
| $B_d^0$ IPs | $< 5.5$ |
| $B_d^0$ FSPV | $> 2.5$ |
| $B_d^0$ $\cos\theta$ | $> 0.9999$ |
| Yield after all triggers | $(1.34 \pm 0.08) \cdot 10^6$ |
| $\frac{S}{B}$ | $4.6 \pm 1.4$ |

of a series of inclusive and exclusive reconstruction algorithms using an identical framework to the full offline selections. The HLT1 stage reduces the event rate from the 1 MHz L0 output rate to 33 kHz, while the HLT2 stage reduces this 33 kHz to the final trigger output rate of 2 kHz.

Since the L0 and HLT triggers are undergoing reoptimization, the precise values of their efficiencies for these decay modes are difficult to quote. Such values have in fact been measured in the full LHCb simulation using various trigger optimizations, but at the time of writing there is no "official" trigger configuration corresponding to the DC06 simulation, so the choice of which numbers to quote is somewhat arbitrary. Throughout this note, a L0 efficiency of 45% will be taken as representative of the likely final L0 trigger performance for these decay modes. No HLT efficiency will be quoted, because the performance of the HLT for these decay modes is not understood well enough at present.

# 5 Offline selection

The existing offline selections [5, 4] for the decay modes $B_{d,s}^0 \to D_{d,s}^{\pm}(\pi, K)^{\mp}$ were already quite similar, so unifying them was a matter of fine tuning the cuts to optimize overall signal yields and purities. The strategy chosen was to first use the same kinematic and decay topology cuts for all channels, while differentiating between the different decay modes by using the appropriate particle ID requirements. The kinematic and decay topology cuts could then be adjusted to achieve the suppression of combinatoric background appropriate to the branching ratio of any given channel, but no new cuts would be introduced. Since the channel $B_d^0 \to D_d^{\pm}\pi^{\mp}$ has the highest branching ratio, it will require the loosest cuts to achieve a desired purity; therefore, it makes sense to begin by optimizing the unified selection for the channel $B_d^0 \to D_d^{\pm}\pi^{\mp}$, and then tighten the cuts as required for the channels $B_s^0 \to D_s^{\pm}K^{\mp}$ and $B_s^0 \to D_s^{-}\pi^{+}$.

The starting point for this study was the existing $B_d^0 \to D_d^{\pm}\pi^{\mp}$ selection, which had been optimized to give the highest sensitivity possible to $\gamma$. Table 2 lists the cuts used. In the DC04 study, this channel had only been optimized on b-inclusive background[3]. In this DC06 study, minimum bias background[4] was also considered, and the cuts were reoptimized for the requirement that zero background candidates are selected in a sample

[3] b-inclusive background events are generated such that each event contains a pair of $b, \bar{b}$ quarks, which hadronize to form bottom mesons and baryons.

[4] Minimum bias events are generated without any prejudice as to the outcome of the $pp$ collision.

of $1.74 \cdot 10^6$ minimum bias events preselected by the L0 trigger. This requirement was chosen as the standard way (across LHCb) of ensuring that offline selections had an acceptably low selection rate on minimum bias events. Controlling this rate is important since it proves that light quark interactions will not constitute an overwhelming background in the decay modes $B^0_{d,s} \to D^{\pm}_{d,s}(\pi, K)^{\mp}$.

Before discussing the reoptimization on minimum bias events, some further explanation of how this selection evolved is required. The minimum bias reoptimization was performed with an early version of the DC06 simulation. The reoptimized selection was subsequently used to estimate signal yields and purities with later versions of the simulation software, whose reconstruction performance was different from the simulation software used for the optimization. The signal yields quoted before and after the reoptimization procedure in Section 5.1 are only meant as a guide to the proportion of the signal yield lost by the reoptimization procedure. The yields and purities quoted in Sections 5.2, 5.3,and 5.4 are the final results of this note.

After the reoptimization on minimum bias events is discussed, the signal yields and purities are estimated for the three channels $B^0_d \to D^{\pm}_d \pi^{\mp}$, $B^0_s \to D^{\pm}_s K^{\mp}$, and $B^0_s \to D^-_s \pi^+$. Note the same sample of b-inclusive background events is used in all three cases when estimating the purity. Other channels in the $B^0_{d,s} \to D^{\pm}_{d,s}(\pi, K)^{\mp}$ family can be selected using the same cuts but changing the PID requirements as appropriate. In particular the Cabibbo surpressed decay modes $D^{\pm}_s \to \pi^{\pm}\pi^{\pm}\pi^{\mp}$ and $D^{\pm}_s \to K^{\pm}\pi^{\pm}\pi^{\mp}$ can be selected in the same manner.[5] The PID cuts for the decay modes $B^0_s \to D^{\pm}_s K^{\mp}$ and $B^0_s \to D^-_s \pi^+$ were copied from the DC04 study [4]. It was felt that showing these cuts to be robust between different versions of the LHCb simulation was more important than reoptimizing them in order to potentially gain some extra efficiency.

## 5.1 Reoptimizing on minimum bias background

### 5.1.1 Starting signal yield

When the cuts listed in Table 2 are applied to a sample of $B^0_d \to D^{\pm}_d \pi^{\mp}$ signal events, the expected yield obtained is $1.37 \cdot 10^6$ signal events in 2 fb$^{-1}$ of data after the L0 trigger.

### 5.1.2 Reoptimization criteria

When the cuts listed in Table 2 are applied to the $1.74 \cdot 10^6$ minimum bias events, seven candidates survive in the tight $B$ mass window. A study of the MC truth content of these events using the Background Category tool [5] shows their content to be:

- Ghost background: Three "ghost" events, in which at least one track used to make the $B$ candidate does not correspond to any physical track left in the detector by a charged particle. These tracks can be a combination of noise, but they can also arise if two charged particles pass close to each other, and their hits are wrongly combined into a single track by the reconstruction software.
- Partially reconstructed physics background: One partially reconstructed decay of a real $B$ hadron.
- Primary vertex background: Two events in which at least one track used to make the $B$ candidate came from the primary vertex.
- $b\overline{b}$ background: One event in which at least one track used to make the $B$ candidate came from the decay of a true $B$ hadron, while no track came from the primary vertex; most likely, the daughters of the two $B$ hadrons were mixed up to form the reconstructed $B$ candidate.

It was therefore necessary to tighten certain cuts in order to select the required zero background candidates. Since an optimization algorithm would likely have struggled to converge properly,[6] this tightening was performed by hand. The goal was to tighten as few cuts as possible, and to lose only $2-3\%$ of signal efficiency for each cut that is tightened. Table 3 lists the cuts tightened and the resulting signal efficiencies. As a result of these cuts, zero candidates survive among $1.74 \cdot 10^6$ minimum bias events, while the expected signal yield obtained is $1.22 \cdot 10^6$ events in 2 fb$^{-1}$ of data after the L0 trigger. The reoptimization loses $\approx 10\%$ of signal events compared to the initial selection. For convenience, the reoptimized offline selection is listed in full in Table 4.

[5] They were not included in this study since no events generated with the LHCb simulation software existed for them, but are important since their combined branching ratio is $\approx 33\%$ of the branching ratio of the Cabibbo favoured decay mode.

[6] It is not only that the starting number of background events, seven, is low; any optimization in which the goal is to select nothing is problematic because of inevitable discontinuities in the efficiency curves.

Table 3: The list of tightened cuts for the channel $B_d^0 \to D_d^{\pm}\pi^{\mp}$. The signal efficiency of each cut with respect to the cut in Table 2 is listed, as well as the cumulative signal efficiency.

| Cut | Cut signal efficiency | Cumulative signal efficiency |
|---|---|---|
| $D^{\pm}$ pion daughter $\pi$ DLL K-Pi $< 5$ | 96% | 96% |
| $D^{\pm}$ daughter IP $\chi^2 > 9$ | 97% | 94% |
| $B_d^0$ IP $\chi^2 < 16$ | 97% | 91% |
| $D^{\pm}$ vertex $\chi^2 < 15$ | 98% | 89% |

Table 4: The list of DC06 reoptimized cuts for the channel $B_d^0 \to D_d^{\pm}\pi^{\mp}$.

| | |
|---|---|
| All particle momenta | $> 2000$ MeV |
| Kaon candidate DLL K-Pi | $> 0$ |
| $D^{\pm}$ pion daughter DLL K-Pi | $< 5$ |
| $D^{\pm}$ daughter $p_t$ | $> 300$ MeV |
| $D^{\pm}$ $p_t$ | $> 2000$ MeV |
| $D^{\pm}$ daughter IP $\chi^2$ | $> 9$ |
| $D^{\pm}$ IP $\chi^2$ | $> 9$ |
| $D^{\pm}$ mass | $\pm 21$ MeV |
| $D^{\pm}$ vertex $\chi^2$ | $< 15$ |
| $D^{\pm}$ FSPV $(\chi^2)$ | $> 100$ |
| Bachelor $\pi$ $p_t$ | $> 500$ MeV |
| Bachelor $\pi$ IP $\chi^2$ | $> 9$ |
| $B_d^0$ mass wide | $\pm 500$ MeV |
| $B_d^0$ mass tight | $\pm 50$ MeV |
| $B_d^0$ vertex $\chi^2$ | $< 10$ |
| $B_d^0$ IP $\chi^2$ | $< 16$ |
| $B_d^0$ FSPV $(\chi^2)$ | $> 6.25$ |
| $B_d^0$ $\cos\theta$ | $> 0.9999$ |

Table 5: The composition of background events surviving in the tight mass window after the reoptimized offline selection for the decay mode $B_d^0 \to D_d^{\pm}\pi^{\mp}$.

| Background category | After final selection |
|---|---|
| Signal | 181 |
| Reflection | 5 |
| Partially reconstructed physics background | 2 |
| Low mass background | 3 |
| Ghost background | 17 |
| $b\overline{b}$ background | 2 |

## 5.2 $B_d^0 \to D_d^{\pm}\pi^{\mp}$ offline yield and purity

Following the reoptimization, the resulting cuts were applied on a sample of $B_d^0 \to D_d^{\pm}\pi^{\mp}$ signal and b-inclusive background events in order to estimate the offline yield and purity. These events were processed with an improved version of the detector simulation and reconstruction software, and the signal yield is therefore substantially higher from the one quoted at the end of the reoptimization procedure.

### 5.2.1 Signal yield

A sample of $1.25 \cdot 10^5$ $B_d^0 \to D_d^{\pm}\pi^{\mp}$ events were used in order to estimate the signal yield. In total, 9388 signal candidates were selected by the reoptimized offline selection before any triggers.

The signal yield is given by

$$\text{Signal} = \frac{N_{sel}}{N_{tot}} \cdot \eta_\theta \cdot f_{\text{had}} \cdot B.R. \cdot 10^{12}. \tag{2}$$

Here, $N_{sel} = 9400 \pm 100$ is the number of events selected on the signal tape; $N_{tot} = 1.25 \cdot 10^5$ is the total number of signal events processed; $\eta_\theta = 0.185$ is the generator-level efficiency for $B_d^0 \to D_d^{\pm}\pi^{\mp}$ signal; $f_{\text{had}} = 0.80$ accounts for the fact that with a hadronization factor of 40%, 80 $B_d^0$ mesons are expected in every 100 $b\overline{b}$ events; $B.R. = (2.47 \pm 0.13) \cdot 10^{-4}$ is the branching ratio for this channel [2]; $10^{12}$ is the number of $b\overline{b}$ events expected in 2 fb$^{-1}$ of data. The signal yield is $(2.75 \pm 0.16) \cdot 10^6$ events in 2 fb$^{-1}$ of data, and its uncertainty is a combination of the uncertainty on the branching ratio and the uncertainty on the number of selected signal events.

As discussed in Section 4, this channel has a L0 efficiency of 45%. The expected signal yield after the offline selection and L0 trigger is therefore $(1.23 \pm 0.08) \cdot 10^6$ events in 2 fb$^{-1}$ of data.

### 5.2.2 b-inclusive background

The reoptimized offline selection was run on $27 \cdot 10^6$ b-inclusive background events to estimate its purity. In total 181 signal and 29 background events are selected in the tight mass window, leading to an approximate purity estimate of $S/B = 6 \pm 1$. As a cross-check, one can calculate the expected background yield in 2 fb$^{-1}$ of data and compare it with the signal yield calculated on the dedicated signal events.

The background yield is given by

$$\text{Background} = \frac{N_{sel}}{N_{tot}} \cdot \eta_\theta \cdot 10^{12}. \tag{3}$$

Here, $N_{sel} = 29$ is the number of background events selected; $N_{tot} = 27 \cdot 10^6$ is the total number of background events processed; $\eta_\theta = 0.43$ is the generator-level efficiency for background; $10^{12}$ is the number of $b\overline{b}$ events expected in one year of LHCb running. This corresponds to a yield of $(0.46 \pm 0.09) \cdot 10^6$ background events in 2 fb$^{-1}$ of data after the full offline selection but before any triggers, and corresponds to $S/B = 6 \pm 1$, consistent with the estimate cited earlier.

The categories of the events selected by the $B_d^0 \to D_d^{\pm}\pi^{\mp}$ offline selection are listed in Table 5. The background is dominated by combinatorics, specifically ghosts. The other substantial contribution to the background level are reflections, events in which a final state particle (here a pion or a kaon) was misidentified. These events are likely $B_d^0 \to D_d^{\pm}K^{\mp}$ decays, where the bachelor kaon was misidentified as a pion.

In total, 19 of the 29 events (ghosts and $b\overline{b}$ background) are combinatorics, corresponding to a combinatoric background yield of $(0.30 \pm 0.08) \cdot 10^6$ events in 2 fb$^{-1}$ of data. The other events can be thought of as "specific"

Table 6: The list of DC06 reoptimized cuts for the channel $B_s^0 \to D_s^- \pi^+$.

| All particle momenta | $> 2000\,\text{MeV}$ |
|---|---|
| All $\pi$ DLL K-Pi | $< 0$ |
| All $\pi$ DLL p-Pi | $< 0$ |
| All $\pi$ DLL mu-Pi | $< 5$ |
| $D_s^\pm$ $K$ daughters DLL K-Pi | $> 0$ |
| $D_s^\pm$ $K$ daughters DLL K-p | $> -10$ |
| $D_s^\pm$ daughter $\mathrm{p}_t$ | $> 300\,\text{MeV}$ |
| $D_s^\pm$ $\mathrm{p}_t$ | $> 2000\,\text{MeV}$ |
| $D_s^\pm$ daughter IP $\chi^2$ | $> 9$ |
| $D_s^\pm$ IP $\chi^2$ | $> 9$ |
| $D_s^\pm$ mass | $\pm 21\,\text{MeV}$ |
| $D_s^\pm$ vertex $\chi^2$ | $< 15$ |
| $D_s^\pm$ FSPV $(\chi^2)$ | $> 100$ |
| Bachelor $\pi$ $\mathrm{p}_t$ | $> 500\,\text{MeV}$ |
| Bachelor $\pi$ IP $\chi^2$ | $> 9$ |
| $B_d^0$ mass wide | $\pm 500\,\text{MeV}$ |
| $B_d^0$ mass tight | $\pm 50\,\text{MeV}$ |
| $B_d^0$ vertex $\chi^2$ | $< 10$ |
| $B_d^0$ IP $\chi^2$ | $< 16$ |
| $B_d^0$ FSPV $(\chi^2)$ | $> 64$ |
| $B_d^0$ $\cos\theta$ | $> 0.9999$ |

background, caused by a genuine $B$ decay that was misidentified or misreconstructed, and are expected to have a yield of $(0.16 \pm 0.05) \cdot 10^6$ events in 2 fb$^{-1}$ of data.

Finally, the L0 trigger is expected to be equally efficient on those background events which pass the full offline selection as it would be on genuine signal events. The expected background yield after the offline selection and L0 trigger is $(0.2 \pm 0.04) \cdot 10^6$ events in 2 fb$^{-1}$ of data.

#### 5.2.3 Specific backgrounds

Since the decay mode $B_d^0 \to D_d^\pm \pi^\mp$ is expected to have a signal yield one order of magnitude greater than any $B_d^0$, $B_s^0$, or $\Lambda_b$ decay with a comparable topology, there are not expected to be any significant specific backgrounds to $B_d^0 \to D_d^\pm \pi^\mp$. The results in Section 5.2.2 confirm this, since the majority of the background events are seen to be combinatorics. It was therefore deemed unnecessary to study specific backgrounds further for this decay mode.

### 5.3 $B_s^0 \to D_s^- \pi^+$

In a similar procedure to that followed for $B_d^0 \to D_d^\pm \pi^\mp$, the reoptimized cuts were applied on a sample of $B_s^0 \to D_s^- \pi^+$ signal and b-inclusive background events in order to estimate the offline yield and purity. Of course, since this decay contains an extra kaon, and proceeds through a different intermediate $D$ state (the $D_s^\pm$ and not the $D_d^\pm$), the cuts used had to be adjusted appropriately. Table 6 lists the final offline selection cuts for the channel $B_s^0 \to D_s^- \pi^+$. A comparison with Table 4 shows that, apart from different particle identification cuts, the flight significance $\chi^2$ cut on the $B$ was tightened from 6.25 to 64. This was necessary since the signal yield is expected to be an order of magnitude below that of $B_d^0 \to D_d^\pm \pi^\mp$; in order to achieve a corresponding decrease in the level of combinatoric background, it is necessary to reconstruct the $B_s^0$ further away from the primary vertex.

#### 5.3.1 Signal yield

A sample of $1.13 \cdot 10^5$ $B_s^0 \to D_s^- \pi^+$ events were used to estimate the signal yield. In total, 6413 signal candidates were selected by the reoptimized offline selection before any triggers.

Table 7: The composition of background events surviving in the tight mass window after the reoptimized offline selection for the decay mode $B_s^0 \to D_s^- \pi^+$.

| Background category | After final selection |
|---|---|
| Signal | 19 |
| Reflection | 4 |
| Ghost background | 2 |
| Primary vertex background | 2 |
| $b\overline{b}$ background | 2 |

The signal yield is given by Equation 2, with $N_{sel} = 6400 \pm 80$; $N_{tot} = 1.13 \cdot 10^5$; $\eta_\theta = 0.185$; $f_{\rm had} = 0.20$; $B.R. = (1.8 \pm 0.5) \cdot 10^{-4}$. The signal yield is $(3.7 \pm 1.0) \cdot 10^5$ events in 2 fb$^{-1}$ of data, and its uncertainty is dominated by that on the branching ratio.

As discussed in Section 4, this channel has a L0 efficiency of 45%. The expected signal yield after the offline selection and L0 trigger is therefore $(1.7 \pm 0.5) \cdot 10^5$ events in 2 fb$^{-1}$ of data.

### 5.3.2 b-inclusive background

A sample of $27 \cdot 10^6$ b-inclusive background events was used to estimate the purity. In total 19 signal and 10 background events are selected in the tight mass window, leading to an approximate purity of $S/B = 2$; a more precise estimate can be obtained by explicitly calculating the expected background yield in 2 fb$^{-1}$ of data and comparing it with the signal yield calculated on the dedicated signal events.

The background yield is given by Equation 3, with $N_{sel} = 10$, $N_{tot} = 27 \cdot 10^6$, and $\eta_\theta = 0.43$. This corresponds to a yield of $(1.6 \pm 0.5) \cdot 10^5$ background events in 2 fb$^{-1}$ of data after the full offline selection but before any triggers, and corresponds to a $S/B$ ratio of $2.3 \pm 0.7$, matching the approximate purity cited earlier.

The categories of the events selected by the $B_s^0 \to D_s^- \pi^+$ offline selection are listed in Table 7. The background is evenly split between combinatorics and genuine, but misidentified, $B$ decays. In total, 6 of the 10 events (ghosts, primary vertex background, and $b\overline{b}$ background) are combinatorics, corresponding to a 90% confidence level (C.L.) Feldman-Cousins (FC) interval [14] of $[0.4, 1.8] \cdot 10^5$ combinatoric background events in 2 fb$^{-1}$ of data before any triggers. The background from genuine $B$ decays will be further explored for several channels of interest in the following section.

Finally, the L0 trigger is expected to be equally efficient on background events which pass the full offline selection as it would be on genuine signal events. The expected background yield after the offline selection and L0 trigger is $(0.7 \pm 0.2) \cdot 10^5$ events in 2 fb$^{-1}$ of data.

### 5.3.3 Specific backgrounds

Unlike $B_d^0 \to D_d^\pm \pi^\mp$, whose branching ratio and the large $B_d^0$ hadronization fraction protect it from most genuine physics backgrounds, the decay $B_s^0 \to D_s^- \pi^+$ is vulnerable to backgrounds from other, misidentified, $b$-hadron decay modes. The most dangerous of these is $B_d^0 \to D_d^\pm \pi^\mp$, since misidentifying a pion daughter of the $D^\pm$ as a kaon can push the reconstructed mass of the $D^\pm$ underneath the $D_s^\pm$ mass peak. In order to obtain a precise estimate of the expected background level from misidentified $b$-hadron decays, four specific background modes were studied:

- $B_d^0 \to D_d^\pm \pi^\mp$: The offline selection for $B_s^0 \to D_s^- \pi^+$ selected 234 events on a sample of $2 \cdot 10^5$ $B_d^0 \to D_d^\pm \pi^\mp$ events. Using Equation 2, the expected background yield in the tight mass window is $(0.43 \pm 0.04) \cdot 10^5$ events in 2 fb$^{-1}$ of data before any triggers.

- $\Lambda_b \to \Lambda_c^+ (pK^-\pi^+)\pi^-$: The offline selection for $B_s^0 \to D_s^- \pi^+$ selected 35 events on a sample of $5.6 \cdot 10^4$ $\Lambda_b \to \Lambda_c^+ \pi^-$ events. Using Equation 2, with $\eta_\theta = 0.185$, $f_{\rm had} = 0.20$, and $B.R. = (4.4 \pm 2.0) \cdot 10^{-4}$, the expected background yield is $(1.0 \pm 0.5) \cdot 10^4$ events in 2 fb$^{-1}$ of data before any triggers. The large uncertainty is dominated by the uncertainty on the branching ratio of this mode. This background can be reduced by applying tighter DLL (K-p) cuts, but the large uncertainty on the branching ratio makes any reoptimization on simulated data a rather academic exercise. The precise values of these cuts will be optimized on real data, when the quantity of this background is understood better.

- $\Lambda_b \to D_s^- p$: The offline selection for $B_s^0 \to D_s^- \pi^+$ selected 47 events on a sample of $5.7 \cdot 10^4$ $\Lambda_b \to D_s^- p$ events. In order to calculate the background yield it is necessary to make an assumption about the

Table 8: The list of DC06 reoptimized cuts for the channel $B_s^0 \to D_s^\pm K^\mp$.

| | |
|---|---|
| All particle momenta | $> 2000$ MeV |
| Bachelor kaon momentum | $< 100$ GeV |
| $D_s^\pm$ $\pi$ daughter DLL K-Pi | $< 5$ |
| $D_s^\pm$ $K$ daughters DLL K-Pi | $> 0$ |
| $D_s^\pm$ $K$ daughters DLL K-p | $> -10$ |
| Bachelor kaon DLL K-Pi | $> 4$ |
| Bachelor kaon DLL K-p | $> 5$ |
| $D_s^\pm$ daughter $p_t$ | $> 300$ MeV |
| $D_s^\pm$ $p_t$ | $> 2000$ MeV |
| $D_s^\pm$ daughter IP $\chi^2$ | $> 9$ |
| $D_s^\pm$ IP $\chi^2$ | $> 9$ |
| $D_s^\pm$ mass | $\pm 21$ MeV |
| $D_s^\pm$ vertex $\chi^2$ | $< 15$ |
| $D_s^\pm$ FSPV $(\chi^2)$ | $> 100$ |
| Bachelor $K$ $p_t$ | $> 500$ MeV |
| Bachelor $K$ IP $\chi^2$ | $> 9$ |
| $B_d^0$ mass wide | $\pm 500$ MeV |
| $B_d^0$ mass tight | $\pm 50$ MeV |
| $B_d^0$ vertex $\chi^2$ | $< 10$ |
| $B_d^0$ IP $\chi^2$ | $< 16$ |
| $B_d^0$ FSPV $(\chi^2)$ | $> 144$ |
| $B_d^0$ $\cos\theta$ | $> 0.9999$ |

branching ratio of this mode, which has never been observed. To do so, we scale the branching ratio of $\Lambda_b \to \Lambda_c^+ \pi^-$ by $|V_{ub}/V_{cb}| \approx 7 \cdot 10^{-3}$ and include the branching ratio for $D_s^\pm \to K^\pm K^\mp \pi^\pm$, obtaining $B.R. = 3.6 \cdot 10^{-6}$. Using Equation 2, with $\eta_\theta = 0.193$, and $f_{\rm had} = 0.20$, the expected background yield is $120 \pm 20$ events in 2 fb$^{-1}$ of data before any triggers and therefore negligable.

- $B_s^0 \to D_s^\pm \mu^\mp \nu$: The offline selection for $B_s^0 \to D_s^- \pi^+$ selected zero events on a sample of $3.8 \cdot 10^5$ $B_s^0 \to D_s^\pm \mu^\mp \nu$ events, which contains all $B_s^0$ decays to a $D_s^\pm \mu^\mp \nu$ final state, including those proceeding through an intermediate $\tau$ decay or an excited $D_s$ state. Using Equation 2, with $\eta_\theta = 0.19$ and $B.R. = (4.4 \pm 1.3) \cdot 10^{-4}$, the upper 90% C.L. FC limit on the background yield is $1 \cdot 10^3$ events in 2 fb$^{-1}$ of data before any triggers.

The major source of specific background will be the decay $B_d^0 \to D_d^\pm \pi^\mp$, but with significant contributions from $\Lambda_b$ decays, which are also dangerous because they make it more difficult to correctly estimate the level of combinatoric background from the upper mass sideband. This highlights the need to keep a mass window open above the $\Lambda_b$ mass, something accomplished by the $\pm 500$ MeV mass window, for combinatoric estimation.

## 5.4 $B_s^0 \to D_s^\pm K^\mp$

The reoptimized cuts were applied on a sample of $B_s^0 \to D_s^\pm K^\mp$ signal and b-inclusive background events in order to estimate the offline yield and purity. Adjustments were made to the PID cuts based on those used in the DC04 study [4]. Table 8 lists the final offline selection cuts for the channel $B_s^0 \to D_s^\pm K^\mp$. Compared to the $B_s^0 \to D_s^- \pi^+$ selection cuts, the flight significance $\chi^2$ criterion on the B was tightened again, from 64 to 144, because the lower branching ratio of the $B_s^0 \to D_s^\pm K^\mp$ decay mode requires even more stringent flight significance cuts to reduce the combinatoric background level. Also, an upper momentum cut is applied on the bachelor kaon, since the RICH detectors used for particle identification in LHCb have limited discriminating power between kaons and pions above $p = 100$ GeV.

### 5.4.1 Signal yield

A sample of $1.55 \cdot 10^4$ $B_s^0 \to D_s^\pm K^\mp$ events were used to estimate the signal yield. In total, 678 signal candidates were selected by the reoptimized offline selection before any triggers.

Table 9: The composition of background events surviving in the wide mass window after the reoptimized offline selection for the decay mode $B_s^0 \to D_s^\pm K^\mp$.

| Background category | After final selection |
|---|---|
| Signal | 1 |
| Fully reconstructed background | 2 |
| Partially reconstructed background | 1 |
| Low mass background | 2 |
| Ghost | 1 |
| Pileup | 1 |

The signal yield is given by Equation 2, with $N_{sel} = 680 \pm 26$; $N_{tot} = 1.55 \cdot 10^4$; $\eta_\theta = 0.19$; $f_{\rm had} = 0.20$; $B.R. = (1.9 \pm 0.7) \cdot 10^{-5}$. The measured signal yield is $(3.1 \pm 1.1) \cdot 10^4$ events in 2 fb$^{-1}$ of data, and its uncertainty is dominated by the large uncertainty on the the branching ratio. As discussed in Section 4, this channel has a L0 efficiency of 45%. The expected signal yield after the offline selection and L0 trigger is therefore $(1.4 \pm 0.5) \cdot 10^4$ events in 2 fb$^{-1}$ of data.

### 5.4.2 B-inclusive background

As before, a sample of $27 \cdot 10^6$ b-inclusive background events was used to estimate the purity. In total no background events are selected in the tight mass window, and seven background events are selected in the wide mass window. The categories of the events selected by the $B_s^0 \to D_s^\pm K^\mp$ offline selection are listed in Table 9. The fully reconstructed background events are $B_d^0 \to D_s^\pm K^\mp$ decays, which will never fall inside the tight mass window. The low mass background will likewise always fall outside the tight mass window, and the level of specific partially reconstructed background will be estimated from dedicated studies as with $B_d^0 \to D_s^\pm \pi^\mp$, so that only the ghost and pileup events remain. The combinatoric background yield is given by Equation 3, with $N_{sel} = 2$; $N_{tot} = 27 \cdot 10^6$; $\eta_\theta = 0.43$. This corresponds to a 90% C.L. FC interval of $[1, 9.5] \cdot 10^3$ combinatoric background events in 2 fb$^{-1}$ of data after the full offline selection but before any triggers. The expected combinatoric background yield (at 90% C.L.) after the offline selection and L0 trigger is $[0.5, 4.3] \cdot 10^3$ events in 2 fb$^{-1}$ of data.

### 5.4.3 Specific backgrounds

The comments made about specific backgrounds for $B_s^0 \to D_s^- \pi^+$ hold true for $B_s^0 \to D_s^\pm K^\mp$ as well, only more so since the branching ratio is even lower. The same four specific background channels were studied, and in addition the background contribution from $B_s^0 \to D_s^- \pi^+$ was estimated.

- $B_d^0 \to D_d^\pm \pi^\mp$: Zero events were selected in the tight mass window on a sample of $2 \cdot 10^5$ $B_d^0 \to D_d^\pm \pi^\mp$ events. The upper 90% C.L. FC limit on the background yield is 450 events in 2 fb$^{-1}$ of data before any triggers.
- $B_s^0 \to D_s^- \pi^+$: 76 events were selected in the tight mass window on a sample of $2.5 \cdot 10^5$ $B_s^0 \to D_s^- \pi^+$ events. The expected background yield is $(2.0 \pm 0.6) \cdot 10^3$ events in 2 fb$^{-1}$ of data before any triggers.
- $\Lambda_b \to D_s^- p$: 28 events were selected on a sample of $5.7 \cdot 10^4$ $\Lambda_b \to D_s^- p$ events. The expected background yield is $70 \pm 15$ events in 2 fb$^{-1}$ of data before any triggers and therefore negligible.
- $\Lambda_b \to \Lambda_c^+ (pK^-\pi^+) \pi^-$: Zero events were selected in the tight mass window on a sample of $5.6 \cdot 10^4$ $\Lambda_b \to \Lambda_c^+ \pi^-$ events. The upper 90% C.L. FC limit on the background yield is 700 events in 2 fb$^{-1}$ of data before any triggers.
- $B_s^0 \to D_s^\pm \mu^\mp \nu$: Zero events were selected in the tight mass window from a sample of $3.8 \cdot 10^5$ $B_s^0 \to D_s^\pm \mu^\mp \nu$ events. The upper 90% C.L. FC limit on the background yield is $1 \cdot 10^3$ events in 2 fb$^{-1}$ of data before any triggers.

The major source of specific background will be the decay $B_s^0 \to D_s^- \pi^+$. Due to large uncertainties on the branching ratios of various modes, and the large uncertainty on the combinatoric background quoted earlier, it is difficult to quote an overall background yield or purity for this channel.

Table 10: A summary of the selection performance for the decay modes $B_d^0 \to D_d^\pm \pi^\mp$, $B_s^0 \to D_s^- \pi^+$, and $B_s^0 \to D_d^\pm K^\mp$ using the final reoptimized DC06 selection cuts. All yields are quoted in 2 fb$^{-1}$ of data and before any triggers. Any numbers quoted as $[x, y]$ refer to a 90% C.L. FC interval. Upper limits quoted are at 90% C.L.

| | $B_d^0 \to D_d^\pm \pi^\mp$ | $B_s^0 \to D_s^- \pi^+$ | $B_s^0 \to D_s^\pm K^\mp$ |
|---|---|---|---|
| Signal yield | $(2.75 \pm 0.16) \cdot 10^6$ | $(3.7 \pm 1.0) \cdot 10^5$ | $3.1 \pm 1.1 \cdot 10^4$ |
| Combinatoric bkg yield | $(0.30 \pm 0.08) \cdot 10^6$ | $[0.4, 1.8] \cdot 10^5$ | $[0.1, 0.95] \cdot 10^4$ |
| Specific bkg yield | $(0.16 \pm 0.05) \cdot 10^6$ | See below | See below |
| $B_d^0 \to D_d^\pm \pi^\mp$ bkg yield | N/A | $(0.43 \pm 0.04) \cdot 10^5$ | $< 450$ |
| $B_s^0 \to D_s^- \pi^+$ bkg yield | N/A | N/A | $(0.2 \pm 0.06) \cdot 10^4$ |
| $B_s^0 \to D_s^\pm \mu^\mp \nu X$ bkg yield | N/A | $< 1000$ | $< 1000$ |
| $\Lambda_b \to \Lambda_c \pi^\mp$ bkg yield | N/A | $(0.1 \pm 0.05) \cdot 10^5$ | $< 700$ |
| $\Lambda_b \to D_s^\pm p^\mp$ bkg yield | N/A | $120 \pm 20$ | $70 \pm 10$ |

### 5.5 Summary of offline selection results

Table 10 summarizes the offline selection performance for the three decay modes in question. Figures 3 and 4 respectively show the $B_d^0$ and $D_d^\pm$ mass resolutions from the decay $B_d^0 \to D_d^\pm \pi^\mp$. Figures 5 and 6 show the same for the $B_s^0$ and $D_s^\pm$ from the decay $B_s^0 \to D_s^- \pi^+$. Double Gaussians are fit in all cases, since single Gaussian fits do not have an acceptable $\chi^2$. For convenience when calculating mass intervals, the reader may approximate to single Gaussian widths of 5.5-6 MeV in the $D_{d,s}^\pm$ case and 16-17 MeV in the $B_{d,s}^0$ case.

The measurements of $\gamma$, $\Delta m_{d,s}$, and $\Delta\Gamma_s$ from these decay modes rely on fits to the time-dependent CP asymmetry, whose precision depends on the propertime resolution for the $B_{d,s}^0$ mesons. Figures 7 and 8 show the $B_d^0$ and $B_s^0$ propertime resolutions: 39 fs and 38 fs respectively.

Finally, Figure 9 shows the $B_d^0 \to D_d^\pm \pi^\mp$ mass peak on the $b$-inclusive sample after the full offline selection.

## 6 Outlook and future studies

The selection presented in this note is a rectangular cut selection, in which each of the discriminating variables is constrained independently of the others, and the final selection is a logical AND of these constraints (cuts). Within these working parameters (this type of selection and the discriminating variables listed in this note), the selection of the decay mode $B_d^0 \to D_d^\pm \pi^\mp$ was optimized [5] within the DC04 LHCb simulation framework to give the highest possible sensitivity to the physics parameter $\gamma$. This optimization was performed using a genetic algorithm, thus automatically taking into account any correlations between the variables being optimized. The reader ought to feel reassured that not only does applying the DC04-optimized cuts blindly within the subsequent DC06 LHCb simulation framework achieve comparable yields and purities for the decay mode $B_d^0 \to D_d^\pm \pi^\mp$, but that applying analogous cuts to the decay modes $B_s^0 \to D_s^- \pi^+$ and $B_s^0 \to D_s^\pm K^\mp$ also yields undiminished performance compared to their DC04 selections. Although the challenges posed by real data will be greater than those posed by an upgrade of the detector simulation, such robustness reinforces the belief that LHCb will be able to analyse these decay modes in the early stages of its data taking, when the detector performance is yet to be precisely understood.

A rectangular cut selection will not generally result in an optimal selection efficiency or purity, however, since the distributions of signal and background in parameter space are not likely to be rectangular. Once the detector performance on real data is well understood, it will be necessary to develop multivariate analyses, for example based on Fisher discriminants or Neural Networks, in order to fully exploit the non-rectangular shapes of the signal and background distributions in parameter space for the purposes of event selection. Such analyses will of course be optimized for the highest possible sensitivity to $\gamma$, and detailed stability studies will be required to demonstrate that the selections have not been overoptimized. In addition it is of course possible, and indeed likely, that additional discriminating variables not considered in this note will be discovered and deployed in the future.

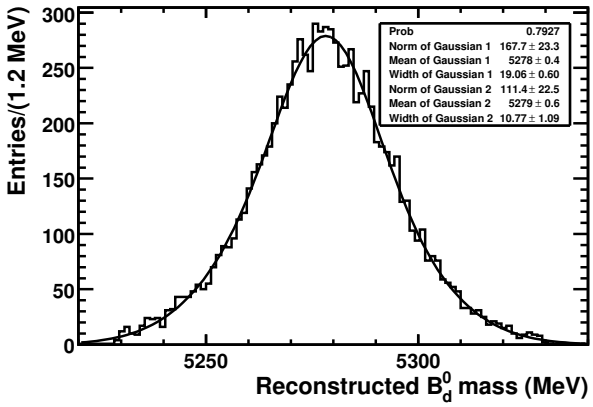


Figure 3: The mass resolution of signal reconstructed $B_d^0$ mesons.

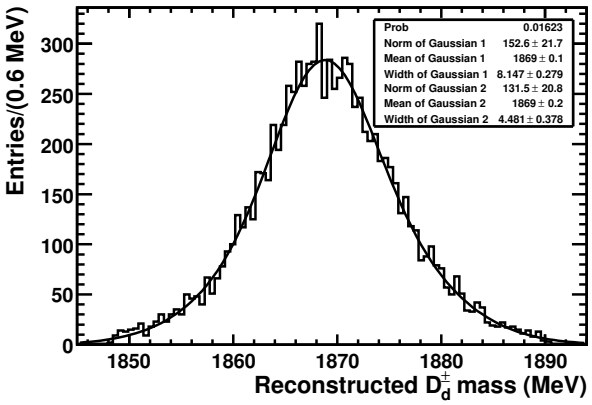


Figure 4: The mass resolution of signal reconstructed $D_d^{\pm}$ mesons.

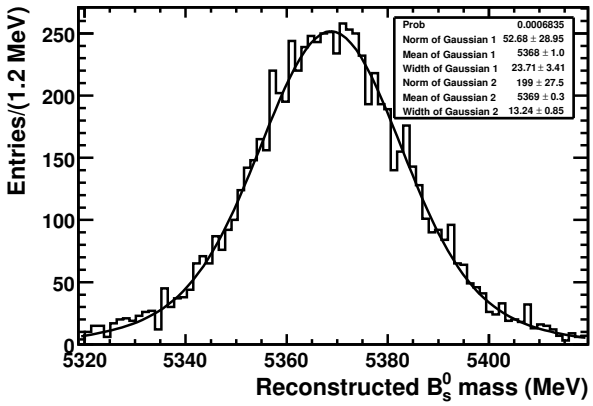


Figure 5: The mass resolution of signal reconstructed $B_s^0$ mesons.

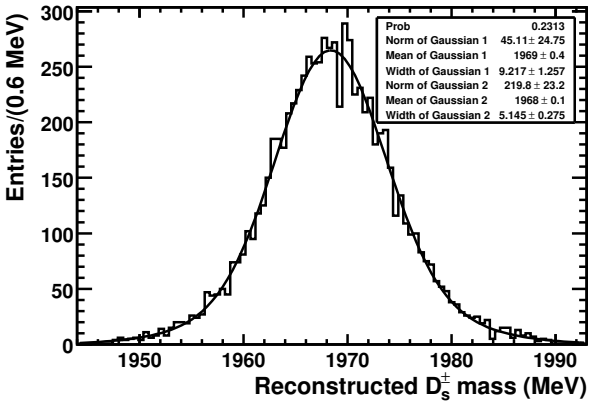


Figure 6: The mass resolution of signal reconstructed $D_s^{\pm}$ mesons.

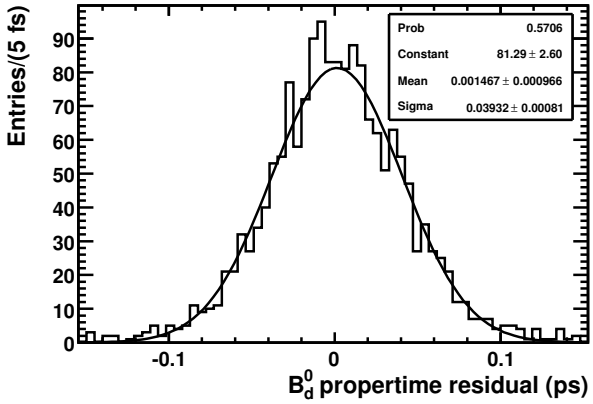


Figure 7: The propertime resolution of signal reconstructed $B_d^0$ mesons.

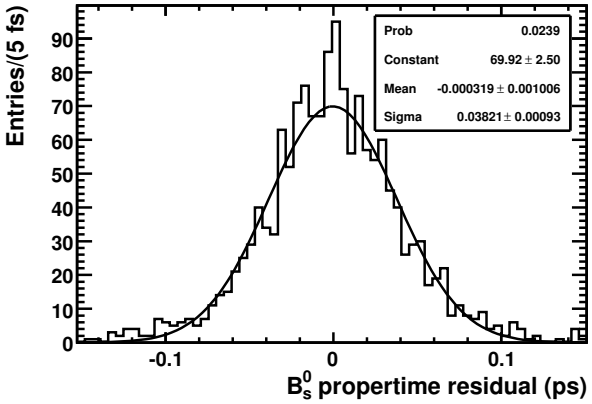


Figure 8: The propertime resolution of signal reconstructed $B_s^0$ mesons.

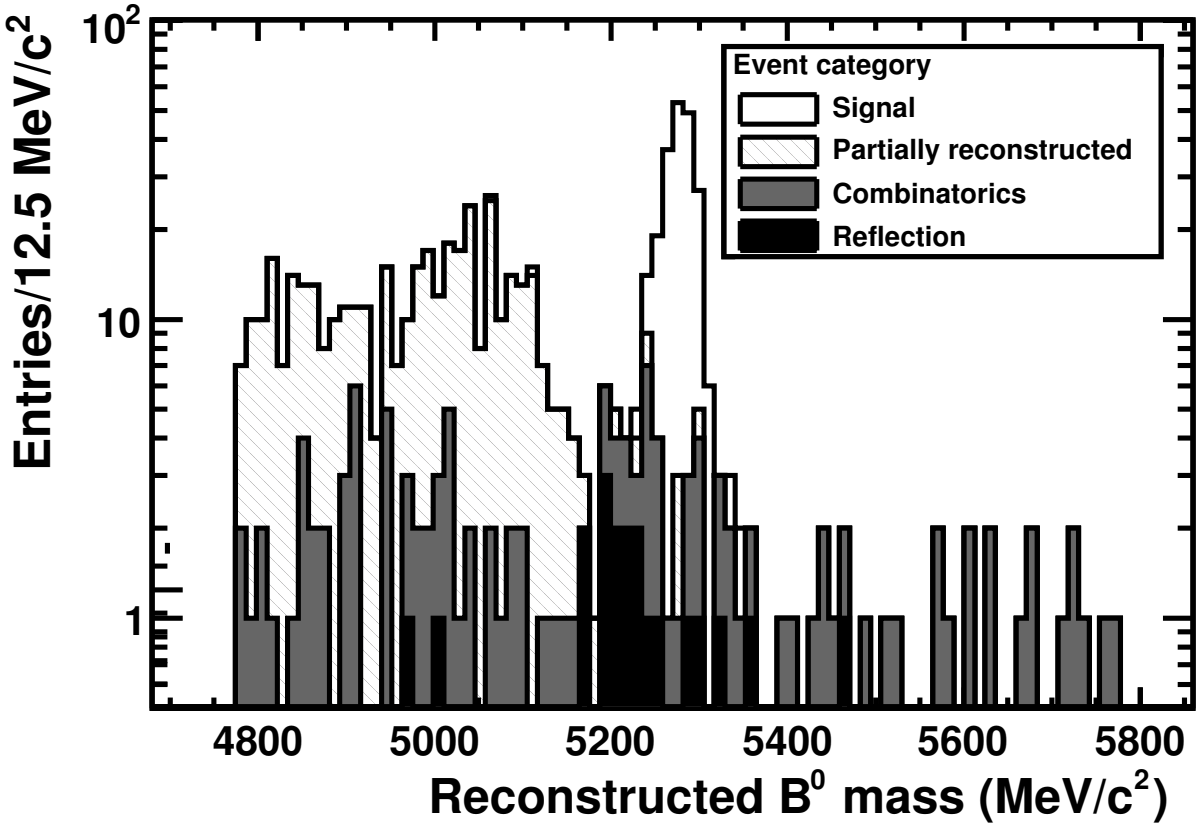


Figure 9: The $B_d^0 \to D_d^{\pm}\pi^{\mp}$ mass peak on the $b$-inclusive simulation sample after the full offline selection. Three different types of backgrounds are distinguished: partially reconstructed background, where a genuine $B$ decay involving a greater number of final state particles was incorrectly reconstructed as $B_d^0 \to D_d^{\pm}\pi^{\mp}$, for example the decay $B_d^0 \to D_d^{\pm}\rho^{\mp}$; combinatoric background, whether from the primary vertex or caused by ghost tracks; and reflections, in which a genuine $B$ decay involving the same number of final state particles was misidentified as $B_d^0 \to D_d^{\pm}\pi^{\mp}$, for example the decay $B_d^0 \to D_d^{\pm}K^{\mp}$.

# 7 Conclusion

A unified approach to the selection of the decay modes $B_{d,s}^0 \to D_{d,s}^{\pm}(\pi, K)^{\mp}$ at the LHCb experiment has been presented. Owing to their identical topologies, all channels are selected with the same set of kinematic cuts; lower branching ratio channels apply a tighter cut on the $B_{d,s}^0$ separation from the primary vertex in order to suppress combinatoric background. Minimum bias, b-inclusive, and specific backgrounds have all been studied, and their contributions to the overall background level in these channels are listed in Table 10. The expected signal yield after the offline selection and L0 trigger in 2 fb$^{-1}$ of data is $(1.23 \pm 0.08)\cdot 10^6$ events for $B_d^0 \to D_d^{\pm}\pi^{\mp}$, $(1.7 \pm 0.5) \cdot 10^5$ events for $B_s^0 \to D_s^-\pi^+$, and $(1.4 \pm 0.5) \cdot 10^4$ events for $B_s^0 \to D_s^{\pm}K^{\mp}$.

# References


[1] J. Muelmenstaedt. First observation of the decay $B_s^0 \to D_s^{\pm} K^{\mp}$ and measurement of the relative branching fraction $B\left(B_s^0 \to D_s^{\pm} K^{\mp}\right) / B\left(B_s^0 \to D_s^- \pi^+\right)$. PhD thesis, 2007. FERMILAB-THESIS-2007-52.

[2] C. Amsler *et al.* (Particle Data Group). *Phys. Lett.*, B667(1), 2008.

[3] A. Golutvin, R. Hierck, J. Van Hunen, M. Prokudin, and R. White. $B_s^0 \to D_s^{\mp} K^{\pm}$ and $B_s^0 \to D_s^{\mp} pi^{\pm}$ event selection. Technical Report CERN-LHCb-2003-127, 2003.

[4] J. Borel, L. Nicolas, O. Schneider, and J. Van Hunen. The $B_s^0 \to D_s^{\mp}\pi^{\pm}$ and $B_s^0 \to D_s^{\mp} K^{\pm}$ selections. Technical Report CERN-LHCb-2007-017, 2007.

[5] V. V. Gligorov. Reconstruction of the Channel $B_d^0 \to D^{\pm}\pi^{\mp}$ and Background Classification at LHCb. Technical Report CERN-LHCb-2007-044, 2007.

[6] G. Wilkinson. Extraction of gamma at LHCb with a Combined $B_s \to D_s^{\pm} K^{\mp}$ and $B_d \to D^{\pm}\pi^{\mp}$ Analysis. Technical Report CERN-LHCb-2005-036, 2005.

[7] V. V. Gligorov and G. Wilkinson. Strategies for measuring $\gamma$ from the decay channels $B_d^0 \to D^{\mp}\pi^{\pm}$ and $B_s^0 \to D_s^{\mp} K^{\pm}$ at LHCb. Technical Report CERN-LHCb-2008-035, 2008.

[8] V. V. Gligorov and J Rademacker. Monte Carlo Independent Lifetime Fitting at LHCb in Lifetime Biased Channels. Technical Report CERN-LHCb-2007-053, 2007.

[9] V. V. Gligorov. Measurement of the CKM angle $\gamma$ and $B$ meson lifetimes at the LHCb detector. PhD thesis, 2008. CERN-THESIS-2008-44.

[10] S. Cohen, M. Merk, and E. Rodrigues. $\gamma + \phi_s$ sensitivity studies from combined $B_s^0 \to D_s^{\mp}\pi^{\pm}$ and $B_s^0 \to D_s^{\mp} K^{\pm}$ samples at LHCb. Technical Report CERN-LHCb-2007-041, 2007.

[11] A. A. Alves Jr. *et al.* The LHCb Detector at the LHC. *JINST*, 3:S08005, 2008.

[12] The LHCb Collaboration. RICH Technical Design Report. 2000. CERN-LHCC-2000-037.

[13] The LHCb Collaboration. LHCb Trigger System Technical Design Report. Technical report, 2003. CERN-LHCC-2003-031.

[14] G. J. Feldman and R. D. Cousins. A Unified Approach to the Classical Statistical Analysis of Small Signals. *Phys. Rev.*, D57:3873–3889, 1998.